

# Badland area Geomorphological Changes

Neelam Devi\*

Qualified NET in Geography in 2019

**Abstract -** Badland formations are an ever-expanding network of erosive channels that make land unsuitable for cultivation and other uses. The Narmada & Sherrivers' alluvium badland trail is situated in India's central region. Using top sheets from the Survey of India (SOI), the area's base map is divided into badland and other land. For morphological characterization, two separate primary badlands have been found. The several map layers for drainage system, contours elevations, distance mapping, isopach (depth of alluvium deposits), & slope are acquired in a GIS environment. According to the study's findings, more than 75% of the badland area's alluvium deposits have been developed. The soft alluvium deposit is a primary reason for the badland's spread onto the alluvium geological area since it is more susceptible to gull erosion. After developing MIE, applying it to the study area, & verifying its accuracy with field data, we may now assess the degree to which badland watersheds are eroded.

**Keywords –** Geomorphologic, Evolution, Badlands, Morphological Parameters

-----X-----

## INTRODUCTION

Naturalists, geomorphologists, and environmental scientists have been fascinated by the breathtakingly austere vistas of the badlands because of the apparent universal destruction shown in these stark or, at most, thinly vegetated regions. In the 18<sup>th</sup> century, initial explorers in North Dakota (USA) used the French expression "mauvaisesterres pour traverser" to describe territories that were difficult to transverse and agriculturally unproductive. Badlands refer to these arid regions (Fairbridge, 1968). Based on these ideas, modern definitions of badlands include landscapes that are extremely fragmented, with hill slopes and divisions produced in loose rock outliers & unconsolidated sediments, little or no vegetation, & unsuitable for farming (Moreno-de las Heras 2016).

The allure of badland habitats can be explained by the fact that the processes that occur there are instantaneous and quick, and that natural occurrences predominate (Gallart et al., 2013a). High drainage densities are common in badlands, resulting in a variety of slopes & ravine formations, alluvium expanses, & washes. This is brought on by surface fluvial processes, piping, & bedrock degradation. They are in charge of many of the landforms & processes that produce more moderate landscapes on a smaller, more limited scale (Campbell, 1989; Howard, 2009). Badlands are characterized by linear erosional features, whereas gully systems feature both hill slopes and splits (Gallart et al., 2002). However, gully growth can initiated or restart badland processes (Nogueras et al., 2000; Ballesteros-Cánovas et al., 2017), hence gully systems are intrinsically linked to badlands.

Badlands are typically unimportant parts of the landscape. For illustration, large-scale area studies reveal that badlands only account for a couple of thousand sq.km in the Mediterranean basin and for about 2.5% of desert landscapes in the southwestern U.S. (Clements et al., 1957). Most people think of badlands as places where a lot of sediment is produced on a regional scale, despite the fact that they often don't cover very much land. A recent meta-analysis of 55 studies on badland erosion in the Mediterranean basin reveals that rates of erosion near to and above 100 t ha<sup>-1</sup> yr<sup>-1</sup> are prevalent at field measurement scales between 104 - 103 ha (Nadal-Romero et al., 2011, 2014a). For habitats further downstream, these high rates of sediment production have significant geomorphological effects. For example, that badlands are necessary for maintaining river deltas and organizing the sedimentary formations of rivers (Clotet, 1984; Grove 2001). However, field observations & modeling studies have shown moderate denudation rates over broad regions at a variety of historical badland sites, proposing that these landscapes may have stayed reasonably constant over the millennia, so tread carefully when discussing the erosive activity of badlands. Daz-Hernández, J., & Juliá, A. (2006) Badlands are extremely fragmented landforms that have certain basic morphological characteristics but can also exhibit a wide range of geomorphic activity & dynamic behavior (Torri et al., 2000; Gallart et al., 2013a;).

Many aspects have been proposed as major contributors to badland formation. Denudation instability occurs when the climate mediates the equilibrium among erosive force & vegetation

management in hillslope, badland systems (Alexander et al., 1994; Bochet et al., 2009). The topographic gradient, subsurface conditions, weather ability & erosion susceptibility of the underlying bedrock are all provided by regional tectonics and lithology, which play a significant role in the formation of badlands (Harvey, 1987; Campbell, 1989; Kasanin-Grubin, 2013). However, they may also manifest in tertiary forms brought on by regional triggers such extreme-event floods or human activities (Wainwright, 1996; Ballesteros-Cánovas et al., 2017). Large swathes of badland can be caused by both regional base-level shift and soft saline bedrocks, which inhibit plant development (Howard, 2009). To better understand the formation of badlands & create a morphological measure of erodibility for equaling the cruelty of erosion across watersheds, the current study examines the geological & river network context of badlands.

### AREAS OF INDIA AFFECTED BY RAVINES

In 1971, India was home to over 3.975% million hectares (ha) of ravines. (NCA, 1976). The area was reduced to 2.678,000 acres as a result of land reclamation efforts that year. (GOI, 1996). But the area of damaged forest has increased from 19.494 million ha in 1971 to 24.897 million ha in 1996. There hasn't been a coordinated, comprehensive survey of the different types of land degradation across the nation by any agency. The data used or provided by different authorities is only based on information gleaned from sporadic sources or general observations. The research conducted by the Natural Bureau of Soil Survey & Land Use Planning (2007) used a map with a scale of 1:1000000. Using soil profile data collected on a 10 km grid, NBBS & LUP generated their soil degradation map (GOI, 1996). The Government of India report (GOI, 1996) indicates a ravine affected area of 2,678,000 ha, an estimate generated after consultation with many authorities. There was no actual fieldwork done to produce these results. Compared to previous projections, it represents, at most, a slight improvement. As of 1971, there were 0.883,000 square kilometers of land in Madhya Pradesh that had been damaged by ravines. In 1996, it shrank to 0.623 million ha (GOI, 1996).

### CLIMATE & LOCATION OF THE STUDY REGION

The developed badland on the alluvium belt may be seen along the Narmada River basin, which includes the river's minor tributaries as well as the confluence of the Sher, Barureva, & Umar rivers (Figure 1). The southern bank of the Narmada River, with its tiny tributaries like the Dhamani & Saras rivers, has been fully devastated by badland development. In contrast, the area where the Sher, Umar, & Barureva rivers all meet the Narmada has developed extensive badland. The Sher River Valley is also somewhat impacted by badland development. Around 22.0049'.00" N, 79.00.00 E and 23.0049.0'50.5"N, 79.00 25.0' 9.20"E is where the alluvium poor land tract along the Narmada & Sher rivers may be found.

The mentioned badland tracts are chosen to assess the local morphology. According to history, the region was a favorite grazing place, and shepherds & nomads built permanent villages there (Tignath et al., 2005). Soils in this area have a loamy texture & contain a little amount of clay. Large seasonal changes in temperature, precipitation, and humidity characterize the subtropical climate of the studied area.

**Rainfall:** The south-west monsoon causes the rainy season, which runs from June through October. In addition, the north-east monsoon provides some precipitation throughout the months of January & February. Rainfall occurs primarily in July & August. Typically, the rain will cease toward the month's end of September. In a few years, though, October saw significant monsoon precipitation, too, averaging 1053 millimeters.

**Temperature:** The study area experiences a sharp increase in temperature from the beginning of March through the hottest month of the year, May. Every day in May, the highest temperature usually reaches between 39 and 45 degrees Celsius. When the monsoon finally arrives in the second week of June, the temperature drops significantly during the day. Temperatures drop quickly day & night starting in mid-November. The winter months of December & January are the coldest. The average annual temperature ranges between 2 and 45 degrees Celsius. Overall, the nights are cooler while the days are warm.

**Relative Humidity:** In the months of July, August, and September, the relative humidity ranges from 83.9 to 89.6% during the morning hours. The months with the lowest morning relative humidity, ranging from 40.3 to 48.6%, are March, April, and May. Morning relative humidity is 60.5% and nighttime relative humidity is 45.6% on average each year.

**Wind Speed:** In the study region (Narsinghpur station), the mean annual wind speed is 2.44 km/h in the morning & 4.35 km/h in the evening. In the months of May and June, which are the pre-monsoon season, the wind speed is at its peak. The month of June has the maximum wind speed of 7.41 km/hr, while the month of January records the lowest wind speed of 2.98 km/hr. In the morning, the average seasonal wind speed is 3.05 km/h, while in the evening, it is 5.96 km/h. Mean wind speeds are seen to be higher in the evenings than they are in the mornings.

The term "potential evapotranspiration" (PET) refers to the quantity of water lost through transpiration by a low-lying crop that casts a constant, even canopy over the ground or never needs to be irrigated. Previous studies have shown that May has the greatest PET levels (200 mm) while December has the lowest (60 mm).

## MATERIAL AND METHODS

Using a topographic survey map, the area's base map was constructed to show how the badlands and other lands are divided (Survey of India, 1972).

### The Badland: A GIS Morphological Study

The morphological characteristics of the 2 badlands—one on the Narmada river & other on the Sher river—has led to their selection. GIS software has been used to build a variety of map overlays (ILWIS 3.0, 2001). There are four different types of GIS map layers: a drainage pattern map, an isopach map, an encroachment distance map, a badland encroachment map with the main river track as source, & digital elevation map (DEM) (Figure 4). The DEM of the study area is used to estimate the slope values of these badlands. The following subsection lists and defines the extracted attributes of map layers that are then employed in the computation of different morphological parameters.

### Morphological Index of Erodibility (MIE)

The severity of the degradation & precise procedures that must be performed to repair the area must be determined for each of the multiple micro watersheds that make up a badland area (a ravine affected area). Researchers have used remote sensing, GIS, and a sediment yield index methodology to prioritize micro watersheds (Chakraborti, 1991). Utilizing a morphological analysis of the watershed, Nookaratnam (2005) selected the micro watersheds that are a part of bigger basins. As per the earlier studies, shape characteristics ( $R_c$ ,  $R_e$ , and  $R_f$ ) show an inverse association with erodibility while linear parameters ( $D_d$ ,  $D_f$ ,  $T$  &  $R_h$ ) support erodibility of watersheds. In order to compare the deterioration of watersheds, Biswas et al. (1999) & Nookaratnam et al. (2005) employed a rating system. Thus, using a ranking system to prioritize a watershed within a certain area is useful. However, it cannot be utilized to quantify the impact of morphology on erodibility. It can be challenging and perplexing to compare watersheds using a variety of criteria. For evaluating the combined influence of many morphological characteristics on erodibility, the MIE, as specified below, has been urbanized in the current work.

$$MIE = (D_d \times D_f \times T \times R_h) / (R_c \times R_e \times R_f)$$

**Drainage density ( $D_d$ ):** The stream order index measures how much water flows through a certain area as a percentage of the basin's total stream length. It is expressed in 'km/km<sup>2</sup>'

$$D_d = \sum_{u=1}^n L_u / A$$

**Drainage frequency ( $D_f$ ):** Horton (1932) suggested that the ratio of the total number of streams in a basin to the basin area be the drainage frequency factor. It is stated in no./km<sup>2</sup>.

$$D_f = \sum_{u=1}^n N_u / A$$

**Texture ratio ( $T$ ):** The texture ratio is the proportion of first-order streams to the basin's circumference. There are  $x$  number of first-order streams per kilometer.

$$T = N_1 / P$$

**Relief ratio ( $R_h$ ):** The relief ratio of a basin is calculated by dividing its total relief ( $H$ ) by its greatest length ( $L_b$ ). It represents the system's latent or wasted energy. The unit of measure is "m/km."

$$R_h = H / L_b$$

### Shape parameters of a basin

Shape parameters ( $R_c$ ,  $R_e$ , &  $R_f$ ) provide a range of values that describe the shape of a watershed (0 to 1). If the value is close to one, either an elongated or nearly round shape is guaranteed. In generally, elongated watersheds exhibit delayed surface runoff, which leads to reduced erosion, & circular watersheds exhibit the opposite.

**Circularity ratio ( $R_c$ ):** Circularity ratio is computed as:

$$R_c = 12.57A / P^2$$

**Form factor ( $R_f$ ):** It defined as the product of the basin area ( $A$ ) & maximum basin length square ( $L_b$ ).

$$R_f = A / L_b^2$$

**Elongation ratio ( $R_e$ ):** The diameters of a circle with the similar surface as the basin divided by the longest length of the basin yields the elongation ratio.

$$R_e = 1.128A^{0.5} / L_b$$

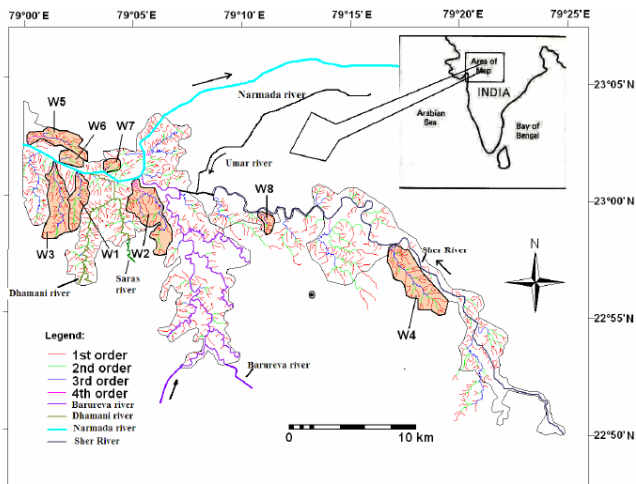


Figure 1: Watershed selection & drainage pattern in a badland area.

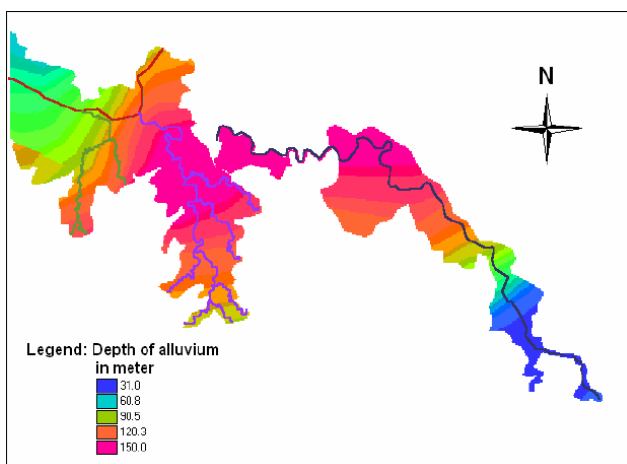


Figure 2: Badland area isopach (alluvium deposit depth)

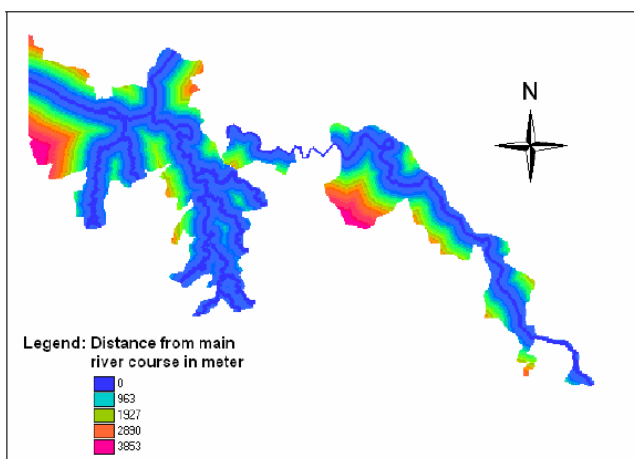


Figure 3: Badland region is encroaching on the main river flow.

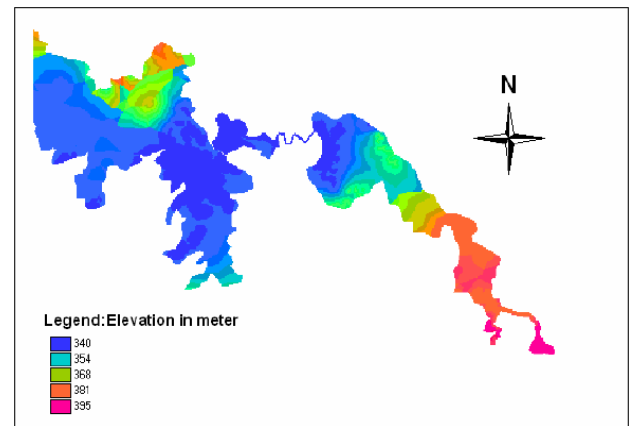


Figure 4: Badland region's DEM.

## RESULTS & DISCUSSION

The pattern, location, & region of badland formation in the research area are all extensively described by the GIS-based analysis of the chosen badland locations. The lengths of the Sher (49.67 km), Barureva (66.26 km), and Dhamani (23.21 km) rivers are found to be slightly impacted by badland formation, whilst the entire Saras river exhibits considerable badland development as it approaches the confluence of the Narmada. The stream network in the Badland area is third- and fourth-ordered (Figure 1).

Related to the badland network of the Sher river ( $A=91.41 \text{ km}^2$ ), the area of badland development is highly dense throughout the Narmada tract, which includes the Barureva, Dhamani, & Saras rivers ( $A=161.53 \text{ km}^2$ ). The particular badlands have virtually equal magnitudes of drainage density & frequency, which are key variables in badland formation, according to a comparison of morphological features (Table 1). However, the Narmada tract's texture ratio is twice that of the Sher badland, making it a significantly damaged badland. Table 2 shows that first order streams account for the majority of the formation of badlands, with the Narmada badlands having the highest percentage (78.46%) compared to the Sher River badlands (64.66%). Based on these findings, the badland situation develops when a high number of first-order streams originate or already exist along the major river water flow.

Table 1: Parameters of the badland area's morphology.

Sl. No.	Morphological parameters	Badland along Narmada river	Badland along Sher river
1.	Area (A), $\text{km}^2$	161.53	91.41
2.	Perimeter (P), km	114.01	111.11
3.	Circularity ratio ( $R_c$ )	0.39	0.31
4.	Drainage density ( $D_d$ ), $\text{km}/\text{km}^2$	2.45	2.22
5.	Drainage frequency ( $D_f$ ), $\text{no.}/\text{km}^2$	4.74	4.74
6.	Texture ratio (T)	5.27	2.52
7.	Relief (H), m	44	70
8.	Average slope (S), %	5.86	3.30
9.	Constant channel maintenance (Cm), $\text{km}^2/\text{km}$	0.41	0.45

Table 2: The badland area's drainage analysis.

Order of stream	Number of streams (N <sub>s</sub> )	Percent to total stream number %	Stream length (L <sub>s</sub> ) km	Percent to total stream length %	Av. stream length (L <sub>s</sub> ) <sub>av</sub> km	Bifurcation ratio (R <sub>b</sub> )	Length ratio (L <sub>s</sub> )
Badland along the selected Narmada river track							
First order	601	78.46	271.03	68.44	0.45	4.32	-
Second order	139	18.14	72.21	18.24	0.52	6.04	1.15
Third order	23	3.00	46.95	11.86	2.04	7.66	3.93
Fourth order	3	0.39	5.82	1.46	1.94	-	0.95
Total/average	766	100	396.01	100.00		(R <sub>b</sub> ) <sub>av</sub> =6.01	(L <sub>s</sub> ) <sub>av</sub> =2.54
Badland along the selected Sher river track							
First order	280	64.66	130.81	64.51	0.46	1.97	-
Second order	142	32.80	45.00	22.19	0.32	14.20	0.68
Third order	10	2.31	25.98	12.81	2.60	10.0	8.20
Fourth order	1	0.23	0.97	0.48	0.96	-	0.37
Total/average	433	100	202.77	100		(R <sub>b</sub> ) <sub>av</sub> =8.72	(L <sub>s</sub> ) <sub>av</sub> =4.43

The distribution patterns of the remaining stream lengths in the two badlands are identical, which strongly supports the contribution of first order streams to the creation of the badlands. The fact that both badlands' reported bifurcation ratio R<sub>b</sub> values are higher than 5.0 indicates that structural control (of the badland process) overrides geomorphic control (Strahler, 1957). The high bifurcation ratios of both badlands & isopach map (Figure 2), which indicates alluvium deposits underground at depths ranging from 30 meters to more than 150 meters, suggest the existence of a flimsy geological foundation. The Sher Badland's wide variety of length ratios suggests that the underlying rock's structure is less uniform. This specifies that the alluvium formation beneath the Sher Badland exhibits vast alluvium deposits of various depths.

Additionally, Figures 5 to 10 show that badland formation is widespread (66.57% area) within 1 km of the main river course. Therefore, it may be inferred that the area where badlands form decreases with increasing distance from the main river flow. Badland encroachment from the main river flow can occur up to 4.6 km away (Figure 3). Figure 2 further demonstrates how badland is found to be invading more heavily in an alluvium geological structures with an alluvium depth of 120 m or more (75% of the region is badland).

Eight watersheds (W1 to W8) around the Narmada & Sherrivers have been chosen for an erodibility analysis (Figure 1). Table 3 compares the morphological characteristics of these 8 watersheds with those of an agricultural watershed. The planned MIE has been determined using Equation (1) & shown in a comparable table for each particular watershed. The range of MIE for the badland watersheds, which denotes the degree of severity, goes from 450 to 7888. The watershed W5 is the most severely damaged and is ranked first, although the watershed W6 is the least severely degraded. To assess the severity and scope of badland watersheds, a nearby agricultural subwatershed that is not affected by badland has been chosen as a reference watershed (W1 to W8). The Umar River Basin, which is close to the badland area, has the least amount of gully erosion and is the most stable location for the reference agriculture watershed (85 U) (Deshmukh et. al, 2009). By examining this reference watershed, 85 U, that generates MIE at 201, it is possible to discriminate between badland watersheds & non-erosive & stable watersheds. If a watershed has a MIE of 201 or less, it can be said to be stable and non-

erosive. With a MIE of 450, or around 225% less than the MIE of the reference watershed, the W6 watershed in the badland region has the lowest MIE ever observed. Therefore, if a watershed in this area has a MIE index that is greater than or equal to 225% of the MIE of the reference watershed, it may be classified as badland. The stable pasture land that is now these badlands was originally close to the main river stream. In terms of slope, soil, and geological structure, badland areas resemble agricultural fields; nevertheless, the presence of active gullies renders them more dissected & unsuitable for agricultural usage.



**Figure 5: The formation of a gully in the W5 sub watershed of the Narmada River.**



**Figure 6: The development of gully cutting along the Narmada River in sub watershed W5.**



**Figure 7: Vertically cutting along the main course of the Sher River.**



**Figure 8: Gullies have been cut vertically in a series along the Sher River's primary channel.**



**Figure 9: Badlands are located along the Sher River's main water.**



**Figure 10: Badland region around Barurevar river in W2 sub watershed**

## CONCLUSION

Badlands were created as a result of the alluvium that accumulated at the Narmada and its tributary confluences over a long period of time due to massive influxes of silt. Another factor in the spread of badland formation is the growth of initial order streams next to the main river water course. The quantity of first order streams created by unmanaged gully erosion is thus critically important to the utility of MIE. Field observations have been used to compare the severity of erosion in micro watersheds using a MIE. If a watershed in the research area has a MIE value that is greater than 2.5 times that of a reference agricultural watershed, that watershed may be considered badland. By utilizing creative watershed solutions like gully filling, stone bunding, & plant strip along the side slope of active gullies, it is possible to restore the badlands & transform them into usable land.

## REFERENCES

1. Alexander, R.W., Harvey, A.M., Calvo-Cases, A., James, P.A., Cerdà, A., 1994. Natural stabilization mechanisms on badland slopes, Tabernas, Almeria, Spain. In: Millington, A.C., Pye, K. (Eds.), *Environmental Change in Drylands: Biogeographical and Geomorphological Perspectives*. Wiley & Sons, Chichester, pp. 85–111.
2. Ballesteros-Cánovas, J.A., Stoffel, M., Martín-Duque, J.F., Corona, C., Lucía, A., Bodoque, J.M., Montgomery, D.R., 2017. Gully evolution and geomorphic adjustments of badlands to reforestation. *Scientific Reports* 7, 45027. <https://doi.org/10.1038/srep45027>.
3. Biswas, S., Sudhakar, S., Desai, V. R., 1999. Prioritization of subwatersheds based on morphometric analysis of drainage basin, A Remote Sensing and GIS approach. *J. of Indian Soc. Remote Sensing*.: 27(3):155-166.
4. Blong, R. J., 1970. The development of discontinuous gullies in a pumice catchment, *Amer. J. Sci.*: 268:369-83.

5. Bochet, E., García-Fayos, P., Poesen, J., 2009. Topographic thresholds for plant colonization on semi-arid slopes. *Earth Surface Processes and Landforms* 34, 1758–1771.
6. Brice, J. C., 1966. Erosion and deposition in the loess-mantled Great Plains, Medicine Creek drainage basin, Nebraska. U.S. Geol. Survey Prof. Paper 352-H: 255-339.
7. Bryan, R.B., Yair, A., 1982. Perspectives on studies of badland geomorphology. In: Bryan, R.B., Yair, A. (Eds.), *Badland Geomorphology and Piping*. Geobooks, Norwich, pp. 1–12.
8. Calvo-Cases, A., Harvey, A.M., 1996. Morphology and development of selected badlands in southeast Spain: implications of climate change. *Earth Surface Processes and Landforms* 21, 725–735.
9. Calvo-Cases, A., Harvey, A.M., Paya-Serrano, J., 1991. Processes, interactions and badland development in SE Spain. In: Bryan, R.B., Yair, A. (Eds.), *Badland Geomorphology and Piping*. Geobooks, Norwich, pp. 75–90.
10. Campbell, I.A., 1989. Badlands and badland gullies. In: Thomas, D.S.G. (Ed.), *Arid Zone Geomorphology*, first ed. Belhaven Press, London, pp. 159–183.
11. Cantón, Y., Domingo, F., Solé-Benet, A., Puigdefábregas, J., 2002. Influence of soil-surface types on the overall runoff of the Tabernas badlands (south-east Spain). *Hydrological Processes* 16, 2621–2643.
12. Charkraborti, A. K., 1991. Sediment yield prediction and prioritization of watershed using remote sensing data. *Proc. 12th Asian Conference on Remote Sensing*, Singapore: pp.Q-3 to Q-3-6.
13. Clements, T., Merriam, R.H., Stone, R.O., Mann Jr., J.F., Eyman, J.L., 1957. A Study of Desert Surface Conditions. Quartermaster Research and Development Command Technical Report EP53. US Army Environmental Protection Research Division, Natick.
14. Clotet, N., 1984. La conca de la Baells (alt Llobregat): Els processos geomorfològics actuals responsables dels subministraments de sòlids i balanç previ de sediments. *Acta Geològica Hispanica* 19, 177–191.
15. Daniels, R. B., 1966. Physiographic history and the soils, entrenched stream systems and gullies, Harrison Co., Iowa. U.S. Dept. Ag. Tech. Bull.: 1348: 51-83.
16. dePloey, J., 1992. Gullying and the age of badlands: an application of the erosional susceptibility model Es. In: Schmidt, K.H., de Ploey, J. (Eds.), *Functional Geomorphology: Landform Analysis and Models*, vol. 23, pp. 31–45 Catena Supplement.
17. Deshmukh, D. S., Chaube, U. C., Tignath, S., 2009. Development of Geomorphological Permeability Index (GPI) for assessment of ground water availability and watershed measures. *Water Resource Management*, Vol 23 (4), DOI 10.1007/s11269-011-9882-2
18. Díaz-Hernández, J.L., Juliá, R., 2006. Geochronological position of badlands and geomorphological patterns in the Guadix-Baza basin (SE Spain). *Quaternary Research* 65, 467–477.
19. Fairbridge, R.W., 1968. *Encyclopedia of Geomorphology*. Reinhold Book Corp., New York.
20. Gallart, F., Clotet, N., 1988. Some aspects of the geomorphic processes triggered by an extreme rainfall event: the November 1982 flood in the eastern Pyrenees. In: Harvey, A.M., Sala, M. (Eds.), *Geomorphic Processes in Environments with Strong Contrasts*, vol. 2, pp. 79–95 *Geomorphic Systems*. Catena Supplement, 13.
21. Gallart, F., Marignani, M., Pérez-Gallego, N., Santi, E., Maccherini, S., 2013a. Thirty years of studies on badlands, from physical to vegetational approaches. A succinct review. *Catena* 106, 4–11.
22. Gallart, F., Solé, A., Puigdefábregas, J., Lázaro, R., 2002. Badland systems in the Mediterranean. In: Bull, J.L., Kirkby, M.J. (Eds.), *Dryland Rivers: Hydrology and Geomorphology of Semi-arid Channels*. Wiley & Sons, Chichester, pp. 299–326.
23. GOI. 1996. Report of working group on soil and water conservation for formation of ninth five year plan, Department of Agriculture and Co-operation, Ministry of Agril., Govt. of India: 35-43.
24. Gregory, K. J., Walling, D.E., 1971. Field measurements in the drainage basin, *Geography* 56: 277-292,
25. Grove, A.T., Rackham, O., 2001. Badlands. In: Grove, A.T., Rackham, O. (Eds.), *The Nature of Mediterranean Europe: An Ecological History*. Yale University Press, New Haven, pp. 271–287.
26. Harvey, A., 1987. Patterns of quaternary aggradation and dissectional landform development in the Almeria region, southeastern Spain: a dry region tectonically-active landscape. *Die Erde* 118, 193–215.
27. Howard, A. D., Kerby, G., 1983. Channel changes in badlands, *Geo.Soc.Am.Bull.*, 94:739-752.
28. Howard, A.D., 1997. Badland morphology and evolution: interpretation using a simulation model. *Earth Surface Processes and Landforms* 22, 211–227.
29. Howard, A.D., 2009. Badlands and gullying. In: Parsons, A.J., Abrahams, A.D. (Eds.), *Geomorphology of Desert Environments*, second ed. Springer, Berlin, pp. 265–299.
30. ILWIS 3.0., 2001. Integrated Land and Water Information System. ILWIS User Guide, ITC, Enschede, The Netherlands, pp. 520.
31. Kasanin-Grubin, M., 2013. Clay mineralogy as a crucial factor in badlands hillslope processes. *Catena* 106, 54–67.
32. Kirkby, M. J., Bull, L. J., 2000. Some factors controlling gully growth in fine-grained sediments: a model applied to South-East Spain. *Catena*, 40:127–146.

33. Kuhn, N., Yair, A., Kasanin-Grubin, M., 2004. Spatial distribution of surface properties, runoff generation and landscape development in the Zin Valley badlands, northern Negev, Israel. *Earth Surface Processes and Landforms* 29, 1417–1430.
34. López-Tarazón, J.A., Batalla, R.J., Vericat, D., Francke, T., 2012. The sediment budget of a highly dynamic mesoscale catchment: the river Isábena. *Geomorphology* 138, 15–28.
35. Moreno-de las Heras, M., Gallart, F., 2016. Lithology controls the regional distribution and morphological diversity of montane Mediterranean badlands in the upper Llobregat basin (Eastern Pyrenees). *Geomorphology* 273, 107–115.
36. Nadal-Romero, E., Martínez-Murillo, J.F., Vanmaercke, M., and Poesen, J., 2014a. Corrigendum to scale-dependency of sediment yield from badland areas in Mediterranean environments. *Progress in Physical Geography* 35 (3), 297–332, (2011). *Progress in Physical Geography* 38, 381–386.
37. Nadal-Romero, E., Martínez-Murillo, J.F., Vanmaercke, M., Poesen, J., 2011. Scale dependency of sediment yield from badland areas in Mediterranean environments. *Progress in Physical Geography* 35, 297–332.
38. NBSS&LUP, 2007. Soils of Madhya Pradesh, Their kinds, distribution, characterization and interpretations for optimizing land use, NBSS Publ.59, soils of India series 6, NBSS&LUP, Nagpur, India. NCA, 1976. Report of National Commission of Agriculture of Government of India.
39. Nogueras, P., Burjachs, F., Gallart, F., Puigdefábregas, J., 2000. Recent gully erosion in the El Cautivo badlands (Tabernas, SE Spain). *Catena* 40, 203–215.
40. Nookaratnam, K., 2005. Check dam positioning by prioritization of micro-watershed using SYI model and morphometric analysis-Remote sensing and GIS perspective. *J. of the Indian Soc. of Remote Sensing*, 30(1):39-61.
41. Pakhmode, V., Kulkarni, H., Deolankar, S. B., 2003. Hydrological-drainage analysis in watershed-programme planning: a case from the Deccan basalt, India. *Hydrogeology Journal*, 11: 595-604.
42. Singh, G., Venkatraman, C., Sastry, G., Joshi, B. P., 1994. *Manual of Soil and Water Conservation Practices*, Third Edition, Oxford and IBP Pub. Co. Pvt. Ltd., New Delhi.
43. Smith, T. R., Bretherton, F. P., 1972. Stability and the conservation of mass in drainage basin evolution. *Water Resources Research*: 1507-1529.
44. Strahler, A. N. 1957. Statistical analysis in geomorphic research. *J. Geol.*, 62:1–25.
45. Thornes, J.B., 1985. The ecology of erosion. *Geography* 70, 222–235.
46. Tignath, S., Chaube, U. C., Mishra, S. K., Awasthi, A. K., 2005. System approach to socio-economic and ecological management of a small badland in Narmada Valley (India), *Proc. of International Conf. on Hydrological Perspectives for Sustainable Development-(HYPSED-2005)*:485-496.
47. Torri, D., Bryan, R.B., 1997. Micropiping processes and biancana evolution in southeast Tuscany. *Geomorphology* 20, 219–235.
48. Torri, D., Calzolari, C., Rodolfi, G., 2000. Badlands in changing environments: an introduction. *Catena* 40, 119–125.
49. Tuckfield, C.G., 1964. Gully Erosion in the New Forest, Hampshire. *Am. J. Sci.* 262:795-807.
50. Wainwright, J., 1996. Hillslope response to extreme storm events: the example of the Vaison-la-Romaine event. In: Anderson, M.G., Brooks, S.M. (Eds.), *Advances in Hillslope Processes*. John Wiley and Sons, Ltd., Chichester, pp. 997–1026.
51. Wainwright, J., Brazier, R.E., 2011. Slope systems. In: Thomas, D.S.G. (Ed.), *Arid Zone Geomorphology: Processes, Form and Change in Drylands*, third ed. Wiley & Sons, Ltd., Chichester, pp. 209–233.
52. Wise, S.M., Thornes, J.B., Gilman, A., 1982. How old are the badlands? A case study from southeast Spain. In: Bryan, R.B., Yair, A. (Eds.), *Badland Geomorphology and Piping*. Geobooks, Norwich, pp. 259–277.
53. Yair, A., Bryan, R.B., Lavee, H., Schwanghart, W., Kuhn, N.J., 2013. The resilience of a badland area to climate change in an arid environment. *Catena* 106, 12–21.
54. Yair, A., Goldberg, P., Brimer, B., 1982. Long term denudation rates in the Zin-Havarim badlands, northern Negev, Israel. In: Bryan, R.B., Yair, A. (Eds.), *Badland Geomorphology and Piping*. Geobooks, Norwich, pp. 279–291.
55. Yair, A., Lavee, H., Bryan, R.B., Adar, E., 1980. Runoff and erosion processes and rates in the Zin valley badlands, northern Negev, Israel. *Earth Surface Processes and Landforms* 5, 205–225.

---

### Corresponding Author

**Student Name\***

Author Designation